CL-220010 Received: January 7, 2022 | Accepted: January 29, 2022 | Web Released: February 3, 2022

Core-shell Metal Oxide Nanowire Array to Analyze Adsorption Behaviors of Volatile Molecules

Wenjun Li,[1,2] Kazuki Nagashima,*[1,3] Takuro Hosomi,[1,3] Jiangyang Liu,[1] Tsunaki Takahashi,[1,3] Guozhu Zhang,[1] Wataru Tanaka,[1] Masaki Kanai,[4] and Takeshi Yanagida*[1,2,4]

[1]*Department of Applied Chemistry, Graduate School of Engineering, The University of Tokyo, 7-3-1 Hongo, Bunkyo-ku, Tokyo 113-8656, Japan*

[2]*Department of Molecular and Material Sciences, Interdisciplinary Graduate School of Engineering Sciences, Kyushu University, 6-1 Kasuga-Koen, Kasuga, Fukuoka 816-8580, Japan*

[3]*PRESTO, Japan Science and Technology Agency, 4-1-8 Honcho, Kawaguchi, Saitama 332-0012, Japan*

[4]*Institute for Materials Chemistry and Engineering, Kyushu University, 6-1 Kasuga-Koen, Kasuga, Fukuoka 816-8580, Japan*

E-mail: kazu-n@g.ecc.u-tokyo.ac.jp (K. Nagashima), yanagida@g.ecc.u-tokyo.ac.jp (T. Yanagida)

We investigated material dependent molecule-to-surface interactions of volatile molecules using a core-shell metal oxide nanowire array. Varying the metal oxide species (ZnO, ZrO_2 and TiO_2), we clearly observed the metal cation dependence on the bonding strength of 2-nonanone. In addition, the quantitative analysis of molecular adsorption amount was successfully performed using the nanowire array. The results highlighted that the core-shell nanowire array provides a foundation for understanding and designing the molecule-to-surface interactions on various applications.

Keywords: Metal oxide nanowire array | Molecular adsorption behaviors | Surface metal cations

Metal oxide nanowires have proven their great promise for applications in chemical sensors, inhomogeneous catalysts, molecular filters and so on, due to not only their thermal/chemical robustness in air and water but also their unique redox properties.[1] Understanding the molecule-to-surface interactions of volatile molecules on metal oxide nanowires is of crucial importance to design the performances of these applications.[2] For their fundamental studies, one of the main interests is the material dependence, and thus many studies have been attempted so far by varying the metal oxide species and/or the dopant species.[3] However, varying the material species frequently involves the morphological changes due to the intrinsic nature of self-assembled nanowire synthesis,[4] which makes difficult quantitative analysis of the molecule-to-surface interactions on various metal oxide nanowire species.

Here we employed core-shell metal oxide nanowire arrays to investigate molecule-to-surface interactions on various nanowire species. Previously our study demonstrated that ZnO nanowire arrays on a substrate successfully revealed the impact of Zn^{2+} on the chemical transformation of volatile aldehyde molecules by amplifying the spectroscopic and spectrometric signals using its huge surface.[5] Also, the benefit of the acquired knowledge was proven in a molecular sensing application.[6] This study applies the nanowire array as a template to form a core-shell nanowire array with various metal oxide species. The core-shell nanowires allow us to alter the metal oxide species while maintaining the nanowire morphology. The well-defined surface area of nanowire array allows us to quantitatively analyze the molecular adsorption amount when comparing with different material species. ZnO, ZrO_2 and TiO_2 were selected in terms of the variations of Lewis acidity and coordination number of composed metal cations. The material dependence of the molecule-to-surface interactions was investigated with these nanowire species using analyte molecule of 2-nonanone, which is known to be a volatile biomarker of *Pseudomonas aeruginosa* in cystic fibrosis and a thermally derived off-flavor compound in milk.[7]

We prepared three nanowire arrays including ZnO nanowires, ZnO/ZrO_2 core-shell nanowires and ZnO/TiO_2 core-shell nanowires. For constructing the core-shell nanowire arrays, firstly a ZnO nanowire array was prepared on SiO_2 coated Si (100) substrate by a seed-assisted hydrothermal method.[8] Ti adhesion layer (5 nm) and ZnO seed layer (100 nm) were deposited on the substrate by radio frequency (RF) sputtering. Aqueous solution for the nanowire growth was prepared by mixing 50 mM zinc acetate dihydrate ($Zn(CH_3COO)_2 \cdot 2H_2O$, Sigma-Aldrich ≥98.0%), 50 mM hexamethylenetetramine ($C_6H_{12}N_4$, Wako 99.0%) and 4.0 g polyethyleneimine (PEI, $M_n \sim 1800$, Sigma-Aldrich 50 wt % in H_2O) in 200 mL deionized (DI) water. The substrate with ZnO seed layer was immersed into the aqueous solution in an upside-down manner to avoid precipitated deposition on the substrate during the nanowire growth. ZnO nanowires were grown using a hydrothermal process at 95 °C for 3–24 h. After the growth, the samples were rinsed with DI water and dried by air flow. For ZnO/ZrO_2 nanowires and ZnO/TiO_2 nanowires, we fabricated the core-shell nanowire heterostructures by depositing the ZrO_2 and TiO_2 shell layers on the ZnO nanowires with RF sputtering at room temperature.[9] For comparison, ZnO/ZnO core-shell nanowires were also fabricated in the same manner. Finally, the samples were annealed at 400 °C in air for 30 min. Another thermal annealing condition was attempted at 800 °C in vacuum (8×10^{-3} Pa) for 30 min to modulate the surface state of ZnO nanowires.[5]

The morphology, the composition and the chemical state of the prepared nanowire arrays were characterized by field emission scanning electron microscope (FESEM) equipped with energy dispersive X-ray spectroscopy (EDS), X-ray photoemission spectroscopy (XPS). The chemical state and the amount of surface adsorbed molecules were evaluated by Fourier transform infrared spectroscopy (FTIR) equipped with an MCT (HgCdTe) detector. The bonding strength of surface-adsorbed molecules was analyzed by temperature programmed desorption (TPD) measurements using gas chromatograph-mass spectrometry (GCMS). Prior to FTIR and GCMS, the analyte 2-nonanone was adsorbed on the sample surface at room temperature in a closed vial filled with saturated vapor. The other detailed conditions of these characterizations are shown in Supporting Information.

 © 2022 The Chemical Society of Japan

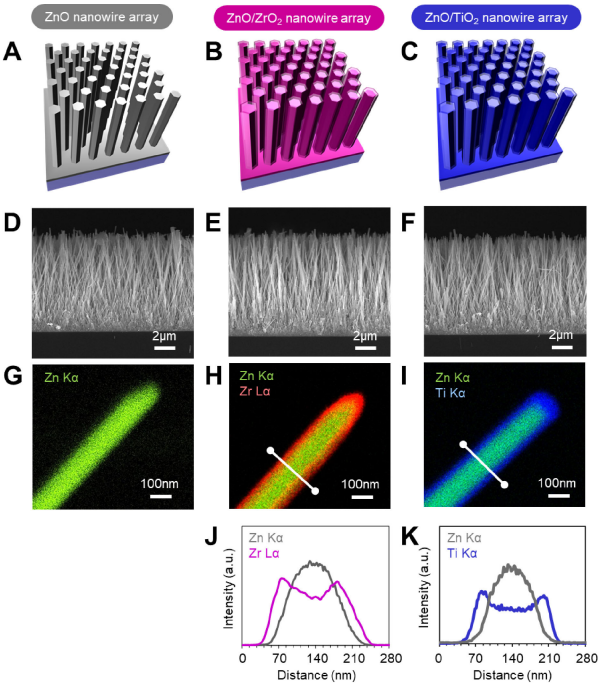

Figure 1. (A–C) Schematic images, (D–F) cross-sectional SEM images, (G–I) EDS elemental mappings and (J, K) elemental line profiles of (A, D, G) ZnO nanowires, (B, E, H, J) ZnO/ZrO_2 nanowires and (C, F, I, K) ZnO/TiO_2 nanowires. For EDS, Zn Kα, Zr Lα and Ti Kα were used.

Firstly, we characterized the morphology of nanowire arrays for ZnO nanowires, ZnO/ZrO_2 nanowires and ZnO/TiO_2 nanowires (Figure 1A–C). The results of morphological characterization by SEM are shown in Figure 1D–F and Figure S1. The nanowires were grown to the out-of-plane direction from the substrate and well spaced from each other. The one-dimensional nanowire growth is due to the preferential [0001]-directed crystal growth of ZnO.[8] The nanowire surfaces were microscopically smooth, and the averaged nanowire diameter was ca. 120 nm for ZnO nanowires and ca. 150 nm for ZnO/ZrO_2 nanowires and ZnO/TiO_2 nanowires. The nanowire length was constant to be ca. 11 μm for the three nanowire samples. The EDS elemental mappings in Figure 1G–I and Figure S2 show that the shell layers were well coated onto the core nanowires with ca. 15 nm thickness. Note that the Zn atom diffusion into the shell layer was negligible (Figure 1J, K). As such, the core-shell metal oxide nanowire arrays were successfully constructed while maintaining their morphology, which offers a reliable platform for investigating a material dependence on the molecule-to-surface interaction.

Next, we characterized the chemical states of metal cations, which may affect the molecule-to-surface interactions.[10] Figure 2 and Figure S3 show XPS spectra for the three nanowire samples. The binding energy (B.E.) values of the observed peaks were respectively 1021.6 eV for Zn $3p_{3/2}$, 181.8 eV for Zr $3d_{5/2}$ and 458.4 eV for Ti $3p_{3/2}$, indicating that the major valence states of metal cations were Zn^{2+}, Zr^{4+} and Ti^{4+} on the three nanowire samples.[11] Figure 2A–C show O1s XPS spectra for the three nanowire samples. In addition to the peaks associated with the lattice oxygen ($O_{lattice}$, B.E. ~529.2–530.1 eV), those

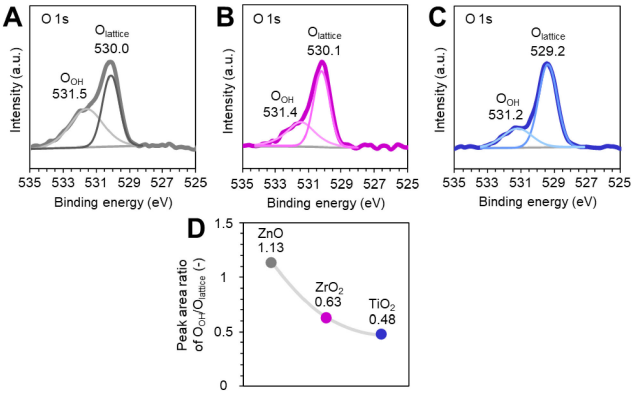

Figure 2. (A–C) O1s XPS spectra of (A) ZnO nanowires, (B) ZnO/ZrO_2 nanowires and (C) ZnO/TiO_2 nanowires. (D) Peak area ratio of $O_{OH}/O_{lattice}$ of the three tested nanowire array.

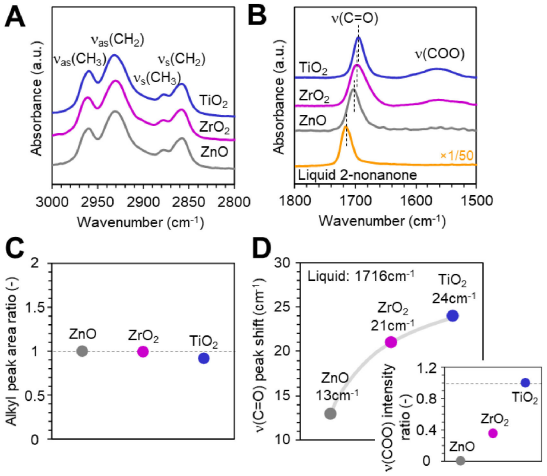

Figure 3. (A, B) FTIR spectra of 2-nonanone adsorbed metal oxide nanowire arrays at (A) alkyl region and (B) carbonyl region. For comparison, a spectrum of liquid concentrate of 2-nonanone is also shown in (B). (C) Alkyl peak area ratio among the three nanowire samples. (D) Degree of peak shift at ν(C=O) compared with liquid concentrate. Inset shows peak intensity ratio of ν(COO) among the three nanowire samples.

associated with the surface hydroxyl group (-OH) (O_{OH}, B.E. ~531.2–531.4 eV) were observed.[5,12] The peak area ratio of $O_{OH}/O_{lattice}$ was 1.13, 0.63 and 0.48 for ZnO nanowires, ZnO/ZrO_2 nanowires and ZnO/TiO_2 nanowires, respectively (Figure 2D). These results showed that more Lewis acid sites (i.e. exposed metal cation sites) exist on ZnO/TiO_2 nanowires and more Brønsted acid sites (i.e. hydroxyl group sites) exist on the ZnO nanowires.

Using the nanowire arrays, we examined the spectroscopic analysis for the molecule-to-surface interactions of 2-nonanone. 2-nonanone (C9 ketone) is known to be a volatile biomarker of *Pseudomonas aeruginosa* in cystic fibrosis and a thermally derived off-flavor compound in milk.[7] Figure 3 shows FTIR spectra of the 2-nonanone adsorbed nanowire samples, where they cover the alkyl region (2800–3000 cm^{-1}: Figure 3A) and the carbonyl/carboxylate region (1500–1800 cm^{-1}: Figure 3B), respectively. As a reference, the spectrum of liquid concentrate

© 2022 The Chemical Society of Japan

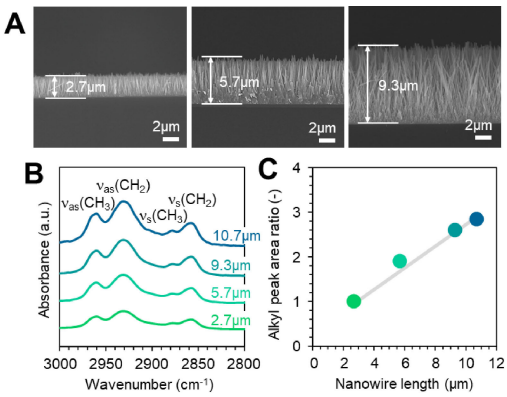

Figure 4. (A) Cross-sectional SEM images of ZnO nanowire arrays with different nanowire length. (B) FTIR spectra (at alkyl region) of ZnO nanowire arrays with different nanowire length. (C) Alkyl peak area ratio when varying the nanowire length.

of 2-nonanone is also shown. In Figure 3A, four peaks assigned as $\nu_{as}(CH_3)$, $\nu_{as}(CH_2)$, $\nu_s(CH_3)$ and $\nu_s(CH_2)$ were observed.[13] Since the alkyl group did not react through the adsorption event, they were utilized as an indicator for evaluating the adsorption amount of 2-nonanone. The nanowire length dependence on molecular adsorption amount indicated that the 2-nonanone was well diffused into the nanowire array (Figure 4). Here, the peak area of alkyl groups was compared among the three nanowire samples (Figure 3C). The results showed that the adsorption amounts of 2-nonanone were quite comparable between the three samples. On the other hand, in Figure 3B, two peaks including the sharp and the broad ones were observed at around 1650–1730 cm^{-1} and 1500–1620 cm^{-1}. These peaks are respectively assigned as ν(C=O) and ν(COO), of which the molecules are coordinated at metal cations (Lewis acid sites).[5,14] Note that any other peaks associated with the coordination at Brønsted acid sites and those of dimer were not observable unlike our previous study of nonanal (C9 aldehyde) adsorption on ZnO nanowires.[5] The presence of ν(COO) peaks indicated that the adsorbed 2-nonanone was partially oxidized. For the ν(C=O) peaks, the peak shift in a comparison with liquid concentrate was consistently seen for the three nanowire samples. We found that both the ν(COO) peak intensity and the degree of peak shift for the ν(C=O) peak tended to be larger in the order of $ZnO < ZrO_2 < TiO_2$ (Figure 3D). The results implied that the molecule-to-surface interaction becomes stronger in this order, and it was coincident with the Lewis acidity of metal cations (Lewis acidity: $Zn^{2+} < Zr^{4+} < Ti^{4+}$).[15] This implication was well supported by the results of TPD measurements in Figure 5, of which the desorption temperatures of adsorbed 2-nonanone on the three nanowire samples increased in the above order. Thus, these results highlighted that the material dependence on the molecule-to-surface interaction was successfully observed using the core-shell nanowire array.

Here we discuss why the 2-nonanone adsorption amounts were comparable between the three nanowire samples with different metal oxide species (Figure 3C). In principle, the molecular adsorption amount might be affected by various factors including the surface area, the adsorption site density, the coordination number and/or the Lewis acidity of metal cations. Note that the influence of surface area difference was not

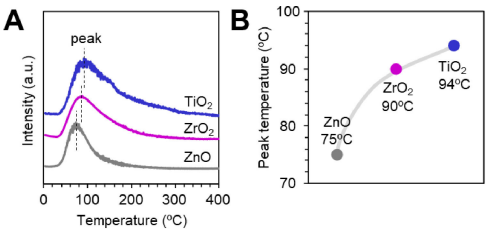

Figure 5. (A) TPD profiles of 2-nonanone adsorbed on the three nanowire samples (at m/z 58). (B) Peak temperatures of TPD profiles in (A).

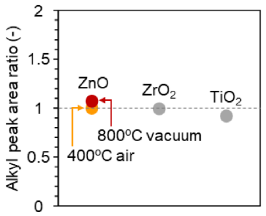

Figure 6. Alkyl peak area ratio when varying the annealing condition. As comparisons, the data of ZnO/ZrO_2 core-shell nanowires and ZnO/TiO_2 core-shell nanowires are also shown.

considerable in our nanowire array as confirmed by the ZnO/ZnO core-shell nanowire array (Figure S4). Also, water in the environment and the surface oxidation event did not significantly influence the adsorption amount (Figure S5 and S6). The results in Figure 3 implied the importance of Lewis acidity and/or Lewis acid site density on the adsorption of 2-nonanone. Since the exposed Lewis acid site density increases in the order of $ZnO < ZrO_2 < TiO_2$ (Figure 2D), we assumed that the effect of adsorption site density was compensated by the other competing factors. In order to reveal the mechanism, we performed the thermal annealing of ZnO nanowires under vacuum to increase the Lewis acid site density by removing the surface hydroxyl groups,[5] and examined its impact on the molecular adsorption amount. Contrary to our expectation, the adsorption amount only slightly increased by annealing, indicating that the adsorption site density does not significantly affect the adsorption amount of 2-nonanone (Figure 6 and Figure S7). These results implied that the adsorbed molecules were plausibly saturated at the nanowire surface. Since 2-nonanone (C9 ketone) is a sterically large molecule, its adsorption at the metal cation site is supposed to be competitive among the molecules even if sufficient adsorption site density is available.[16] Such obtained implications would be beneficial to design a molecular sensing device, i.e. both a sufficient sensing response and a fast recovery are expected in 2-nonanone sensing by employing the metal oxide nanowires composed of metal cation species with relatively weak Lewis acidity.

In conclusion, we investigated the material dependence on the molecule-to-surface interactions of 2-nonanone using a core-shell metal oxide nanowire array. The core-shell nanowire array allowed us to alter the surface metal oxide species while maintaining the nanowire morphology. Spectroscopic and spectrometric analyses revealed that the Lewis acidity of metal cations give a strong impact on the bonding strength of 2-nonanone but not on the adsorption amount. The obtained

© 2022 The Chemical Society of Japan

implications would be beneficial for designing the performance of various metal oxide nanowire-based applications. Thus, this study highlights that the core-shell nanowire array provides a foundation for understanding and designing the molecule-to-surface interactions on various applications.

This work was supported by KAKENHI (Grant No. JP18H01831, JP18H05243, JP20H02208, JP21K18868, JP21K14475), PRESTO Program (Grant No. JPMJPR19J7) of Japan Science and Technology Corporation (JST), and Nanotechnology Platform project of MEXT (A-21-UT-0216). T.Y. was supported by JST CREST (Grant No. JPMJCR19I2) and the Cooperative Research Programs of "Dynamic Alliance for Open Innovation Bridging Human, Environment and Materials in Network Joint Research Center for Materials and Devices", "Network Joint Research Center for Materials and Devices". K.N. acknowledges JACI Prize for Encouraging Young Researcher. XPS measurements were performed at the Center of Advanced Instrument Analysis, Kyushu University and Nanotechnology Platform at The University of Tokyo.

Supporting Information is available on https://doi.org/10.1246/cl.220010.

References

1 Z. Zhou, C. Lan, R. Wei, J. C. Ho, *J. Mater. Chem. C* **2019**, *7*, 202; G. Zhang, H. Zeng, J. Liu, K. Nagashima, T. Takahashi, T. Hosomi, W. Tanaka, T. Yanagida, *Analyst* **2021**, *146*, 6684; H. C. Song, G. R. Lee, K. Jeon, H. Lee, S. W. Lee, Y. S. Jung, J. Y. Park, *ACS Nano* **2020**, *14*, 8335; D. Wang, B. Zhu, X. He, Z. Zhu, G. Hutchins, P. Xu, W.-N. Wang, *Environ. Sci.: Nano* **2018**, *5*, 1096.

2 Y. Ren, W. Xie, Y. Li, J. Ma, J. Li, Y. Liu, Y. Zou, Y. Deng, *ACS Cent. Sci.* **2021**, *7*, 1885; P. Bandyopadhyay, R. Jana, K. Bhattacharyya, O. I. Lebedev, U. Dutta, U. Sarkar, A. Detta, M. M. Seikh, *New J. Chem.* **2019**, *43*, 16621; J. Wang, Z. Li, Z. Gu, *Sens. Actuators Rep.* **2021**, *3*, 100029; G. Zhang, T. Hosomi, W. Mizukami, J. Liu, K. Nagashima, T. Takahashi, M. Kanai, T. Sugiyama, T. Yasui, Y. Aoki, Y. Baba, J. C. Ho, T. Yanagida, *J. Mater. Chem. A* **2021**, *9*, 5815.

3 H. Zeng, G. Zhang, K. Nagashima, T. Takahashi, T. Hosomi, T. Yanagida, *Chemosensors (Basel)* **2021**, *9*, 41.

4 A. Klamchuen, M. Suzuki, K. Nagashima, H. Yoshida, M. Kanai, F. Zhuge, Y. He, G. Meng, S. Kai, S. Takeda, T. Kawai, T. Yanagida, *Nano Lett.* **2015**, *15*, 6406; J. Liu, K. Nagashima, H. Yamashita, W. Mizukami, J. Uzuhashi, T. Hosomi, M. Kanai, X. Zhao, Y. Miura, G. Zhang, T. Takahashi, M. Suzuki, D. Sakai, B. Samransuksamer, Y. He, T. Ohkubo, T. Yasui, Y. Aoki, J. C. Ho, Y. Baba, T. Yanagida, *Commun. Mater.* **2020**, *1*, 58.

5 C. Wang, T. Hosomi, K. Nagashima, T. Takahashi, G. Zhang, M. Kanai, H. Zeng, W. Mizukami, N. Shioya, T. Shimoaka, T. Tamaoka, H. Yoshida, S. Takeda, T. Yasui, Y. Baba, Y. Aoki, J. Terao, T. Hasegawa, T. Yanagida, *Nano Lett.* **2019**, *19*, 2443.

6 C. Wang, T. Hosomi, K. Nagashima, T. Takahashi, G. Zhang, M. Kanai, H. Yoshida, T. Yanagida, *ACS Appl. Mater. Interfaces* **2020**, *12*, 44265; J. Liu, K. Nagashima, Y. Nagamatsu, T. Hosomi, H. Saito, C. Wang, W. Mizukami, G. Zhang, B. Samransuksamer, T. Takahashi, M. Kanai, T. Yasui, Y. Baba, T. Yanagida, *Chem. Sci.* **2021**, *12*, 5073.

7 S. U. Savelev, J. D. Perry, S. J. Bourke, H. Jary, R. Taylor, A. J. Fisher, P. A. Corris, M. Petrie, A. D. Soyza, *Lett. Appl. Microbiol.* **2011**, *52*, 610; P. A. Vazquez-Landaverde, G. Velazquez, J. A. Torres, M. C. Qian, *J. Dairy Sci.* **2005**, *88*, 3764.

8 Y. He, T. Yanagida, K. Nagashima, F. Zhuge, G. Meng, B. Xu, A. Klamchuen, S. Rahong, M. Kanai, X. Li, M. Suzuki, S. Kai, T. Kawai, *J. Phys. Chem. C* **2013**, *117*, 1197; D. Sakai, K. Nagashima, H. Yoshida, M. Kanai, Y. He, G. Zhang, X. Zhao, T. Takahashi, T. Yasui, T. Hosomi, Y. Uchida, S. Takeda, Y. Baba, T. Yanagida, *Sci. Rep.* **2019**, *9*, 14160; X. Zhao, K. Nagashima, G. Zhang, T. Hosomi, H. Yoshida, Y. Akihiro, M. Kanai, W. Mizukami, Z. Zhu, T. Takahashi, M. Suzuki, B. Samransuksamer, G. Meng, T. Yasui, Y. Aoki, Y. Baba, T. Yanagida, *Nano Lett.* **2020**, *20*, 599; Q. Liu, T. Yasui, K. Nagashima, T. Yanagida, M. Hara, M. Horiuchi, Z. Zhu, H. Takahashi, T. Shimada, A. Arima, Y. Baba, *J. Phys. Chem. C* **2020**, *124*, 20563.

9 K. Nagashima, T. Yanagida, H. Tanaka, S. Seki, A. Saeki, S. Tagawa, T. Kawai, *J. Am. Chem. Soc.* **2008**, *130*, 5378; K. Nagashima, T. Yanagida, K. Oka, M. Kanai, A. Klamchuen, J.-S. Kim, B. H. Park, T. Kawai, *Nano Lett.* **2011**, *11*, 2114; K. Nagashima, T. Yanagida, K. Oka, M. Taniguchi, T. Kawai, J.-S. Kim, B. H. Park, *Nano Lett.* **2010**, *10*, 1359.

10 N. C. Jeong, J. S. Lee, E. L. Tae, Y. J. Lee, K. B. Yoon, *Angew. Chem., Int. Ed.* **2008**, *47*, 10128; D. Degler, U. Weimar, N. Barsan, *ACS Sens.* **2019**, *4*, 2228; O. Lupan, V. Postica, J. Gröttrup, A. K. Mishra, N. H. de Leeuw, J. F. C. Carreira, J. Rodrigues, N. B. Sedrine, M. R. Correia, T. Monteiro, V. Cretu, I. Tiginyanu, D. Smazna, Y. K. Mishra, R. Adelung, *ACS Appl. Mater. Interfaces* **2017**, *9*, 4084.

11 M. C. Biesinger, L. W. M. Lau, A. R. Gerson, R. S. C. Smart, *Appl. Surf. Sci.* **2010**, *257*, 887; D. D. Sarma, C. N. R. Rao, *J. Electron Spectrosc. Relat. Phenom.* **1980**, *20*, 25.

12 J.-K. An, N.-K. Chung, J.-T. Kim, S.-H. Hahm, G. Lee, S. B. Lee, T. Lee, I.-S. Park, J.-Y. Yun, *Materials (Basel)* **2018**, *11*, 386; C. Fan, C. Chen, J. Wang, X. Fu, Z. Ren, G. Qian, Z. Wang, *Sci. Rep.* **2015**, *5*, 11712.

13 P. Larkin, **2011**. *Infrared and Raman spectroscopy; principles and spectral interpretation.* Amsterdam Elsevier.

14 M. D. Hernández-Alonso, I. Tejedor-Tejedor, J. M. Coronado, M. A. Anderson, *Appl. Catal., B* **2011**, *101*, 283; T. Komanoya, K. Nakajima, M. Kitano, M. Hara, *J. Phys. Chem. C* **2015**, *119*, 26540; Z. Topalian, B. I. Stefanov, C. G. Granqvist, L. Österlund, *J. Catal.* **2013**, *307*, 265.

15 O. C. Gagné, F. C. Hawthorne, *Acta Crystallogr., B: Struct. Sci. Cryst. Eng. Mater.* **2017**, *73*, 956.

16 D. Talbot, J. Q. Campos, B. L. Checa-Fernandez, J. A. Marins, G. Lomenech, C. Hurel, G. D. Godeau, M. Raboisson-Michel, G. Verger-Dubois, L. Obeid, P. Kuzhir, A. Bee, *ACS Omega* **2021**, *6*, 19086; R. Yamaguchi, T. Hosomi, M. Otani, K. Nagashima, T. Takahashi, G. Zhang, M. Kanai, H. Masai, J. Terao, T. Yanagida, *Langmuir* **2021**, *37*, 5172.

© 2022 The Chemical Society of Japan